

GRASP: GROUP-SHAPLEY FEATURE SELECTION FOR PATIENTS

Yuheng Luo¹, Shuyan Li², Zhong Cao^{3,*}

¹Chinese Academy of Medical Sciences & Peking Union Medical College, Beijing, China

²Queen’s University, Belfast, United Kingdom. ³Heidelberg University, Heidelberg, Germany.

*Email: zhong.cao@uni-heidelberg.de

ABSTRACT

Feature selection remains a major challenge in medical prediction, where existing approaches such as LASSO often lack robustness and interpretability. We introduce GRASP, a novel framework that couples Shapley value driven attribution with group L_{21} regularization to extract compact and non-redundant feature sets. GRASP first distills group level importance scores from a pretrained tree model via SHAP, then enforces structured sparsity through group L_{21} regularized logistic regression, yielding stable and interpretable selections. Extensive comparisons with LASSO, SHAP, and deep learning based methods show that GRASP consistently delivers comparable or superior predictive accuracy, while identifying fewer, less redundant, and more stable features.

Index Terms— shapley values, feature selection, mortality prediction

1. INTRODUCTION

With the growth of electronic health records, medical imaging, and wearable devices, healthcare systems are generating vast amounts of phenotypic data that capture patients’ clinical characteristics, disease manifestations, and treatment responses. These data offer great potential for precision medicine, but their high dimensionality and noise pose major challenges for knowledge discovery [1]. Feature selection is essential as it reduces computational costs by enabling the extraction of the most informative variables.

Feature selection methods are typically categorized as filter, wrapper, and embedded approaches [2, 3, 4]. Filter methods score features using statistical or information-theoretic criteria, offering speed and scalability but often ignoring inter-feature interactions and redundancy [5]. Wrappers evaluate feature subsets via model performance, achieving higher accuracy at significant computational cost [6, 7]. Embedded methods integrate selection into model training, with L1-norm regularization (e.g., LASSO [8], Graphical Lasso [9]) and tree-based models [10]) being widely applied. Recent studies have also focused on developing specific scoring functions to evaluate the consistency and reliability of feature

rankings [11]. Furthermore, another study [12] that exhaustively compares selection methods reveals that the choice of a selector can dramatically affect the final set of variables. Despite advances, existing approaches remain unstable, redundant, and often lack biological interpretability [13]. Moreover, most studies emphasize predictive accuracy while overlooking interpretability and clinical relevance—two requirements critical for medical adoption [14]. Post-hoc explanation tools such as SHAP provide insights, but their outputs may difficult to align with disease-specific mechanisms.

To address these challenges, we propose GRASP (GRoupshApley feature Selection for Patients), an interpretable feature selection algorithm that integrates cross-entropy with SHAP-based attribution into a penalized framework. Unlike prior methods that separate prediction and interpretability, GRASP unifies both to achieve stable selection and clinically meaningful insights. Our main contributions are:

1. **Interpretable framework.** We are the first to couple SHAP-based feature attribution with regularization, enabling optimization algorithms to preserve clinically interpretable features.
2. **Grouped selection mechanism.** We design a group-based strategy that simplifies models and enhances stability and generalization.
3. **Comprehensive evaluation.** This study evaluates feature-selection methods beyond accuracy, offering valuable guidance for the future development of feature selection techniques.

2. METHOD

2.1. Overview

We propose GRASP, a feature selection method that integrates model-derived attributions with group- L_{21} regularized logistic regression, optimized via a proximal-gradient algorithm with Armijo backtracking [15]. The procedure consists of: (1) feature importance calculation; (2) loss function construction; and (3) proximal-gradient optimization. Formally, let $X \in \mathbb{R}^{n \times p}$ be the design matrix with binary outcome $y \in \{0, 1\}^n$, and partition features into G disjoint groups

$\mathcal{G} = g_1, \dots, g_G$. β_g denotes the subvector for group g with Euclidean norm $\|\beta_g\|_2$. Feature importance is ϕ_j , and aggregated group importance is s_g . Fig 1 shows the main workflow of GRASP.

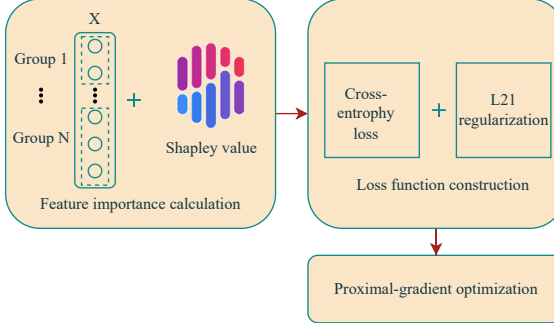


Fig. 1: Workflow of GRASP algorithm. The procedure begins with feature importance calculation by combining input feature groups with Shapley values. These importance scores are then incorporated into a loss function that integrates L_{21} loss and group-wise L_{21} regularization. The final optimization is performed using a proximal-gradient algorithm.

2.2. Feature importance calculation

Given an XGBoost classifier trained on the training fold, compute SHAP values on the held-out validation fold X^{val} . For each feature j and sample i let SHAP_{ij} be the corresponding Shapley value, which is defined as:

$$\phi_j = \frac{1}{n_{\text{val}}} \sum_{i=1}^{n_{\text{val}}} |\text{SHAP}_{ij}|. \quad (1)$$

For each group g we aggregate by the mean of its member feature importances:

$$s_g = \frac{1}{|g|} \sum_{j \in g} \phi_j. \quad (2)$$

The group feature selection strategy in this equation allows highly correlated features to enter or leave together to some extent, enhancing the stability of our feature selection method. Meanwhile, the incorporation of SHAP values ensures that the selected features are more contributive and, consequently, easier to interpret.

To obtain positive group penalty coefficients that decrease with greater importance, we transform s_g into weights:

$$\tilde{\omega}_g = \exp(-s_g/\tau_0) + \varepsilon, \quad \omega_g = \frac{\tilde{\omega}_g}{\sum_{h=1}^G \tilde{\omega}_h}, \quad (3)$$

where τ_0 is an optional scaling parameter (set to 1 by default) and $\varepsilon > 0$ a small constant for numerical stability. This ensures $\omega_g > 0$ and $\sum_g \omega_g = 1$. Intuitively, groups with larger

SHAP scores s_g receive smaller ω_g and thus a reduced multiplicative penalty in the group regularizer.

2.3. Loss function construction

We then fit our loss function with a group L_{21} penalty. The loss is defined as

$$\begin{aligned} \mathcal{L}(\beta) = -\frac{1}{n} \sum_{i=1}^n & \left[y_i \log \sigma(x_i^\top \beta) \right. \\ & \left. + (1 - y_i) \log(1 - \sigma(x_i^\top \beta)) \right], \end{aligned} \quad (4)$$

where $\sigma(z) = (1 + e^{-z})^{-1}$ is the sigmoid. The regularized objective is

$$J(\beta) = \mathcal{L}(\beta) + \lambda \sum_{g=1}^G \omega_g \|\beta_g\|_2, \quad (5)$$

with $\lambda > 0$ the global regularization parameter and ω_g defined in Eq. (3). The penalty term $\Omega = \sum_g \omega_g \|\beta_g\|_2$ enforces group-level sparsity while allowing dense coefficients within selected groups. The key tuning parameter is the regularization weight λ . We adopt a two-step strategy inspired by Gordon's Theorem [16]: after normalization, we compute the empirical noise matrix $E = X^{\text{train}} - \mathbf{1}\bar{X}^\top$ and set λ to $\text{sd}(E)$.

2.4. Proximal-gradient optimization

We optimize Eq. (5) using a proximal-gradient scheme. Given iterate $\beta^{(k)}$ and step-size $t_k > 0$, the update is

$$v_{k+1} = \beta^{(k)} - t_k \nabla \mathcal{L}(\beta^{(k)}), \quad (6)$$

$$\beta^{(k+1)} = \text{prox}_{t_k \lambda \Omega}(v_{k+1}), \quad (7)$$

where the proximal operator for the group L_{21} penalty acts group-wise:

$$\text{prox}_{\tau \omega_g \|\cdot\|_2}(v_g) = \begin{cases} \left(1 - \frac{\tau \omega_g}{\|v_g\|_2}\right) v_g, & \text{if } \|v_g\|_2 > \tau \omega_g, \\ \mathbf{0}, & \text{otherwise,} \end{cases} \quad (8)$$

with $\tau = t_k \lambda$.

An Armijo-type backtracking line-search is employed to select the step-size t_k . Specifically, based on the descent lemma for smooth functions, we accept t_k if

$$\begin{aligned} \mathcal{L}(\beta^{(k+1)}) \leq & \mathcal{L}(\beta^{(k)}) + \nabla \mathcal{L}(\beta^{(k)})^\top (\beta^{(k+1)} - \beta^{(k)}) \\ & + \frac{1}{2t_k} \|\beta^{(k+1)} - \beta^{(k)}\|_2^2, \end{aligned} \quad (9)$$

which ensures sufficient decrease of the objective. If the condition is not satisfied, the step-size is reduced by $t_k \leftarrow \alpha t_k$ with $\alpha \in (0, 1)$ (we use $\alpha = 0.5$), and the test is repeated. The algorithm terminates when $\|\beta^{(k+1)} - \beta^{(k)}\|_2 < \varepsilon$ or a maximum number of iterations is reached.

Finally, we compute the group norms $\|\beta_g\|_2$ and retain the groups satisfying

$$\hat{\mathcal{G}} = g : \|\beta_g\|_2 > 0. \quad (10)$$

All features outside the selected groups are discarded.

3. EXPERIMENTS

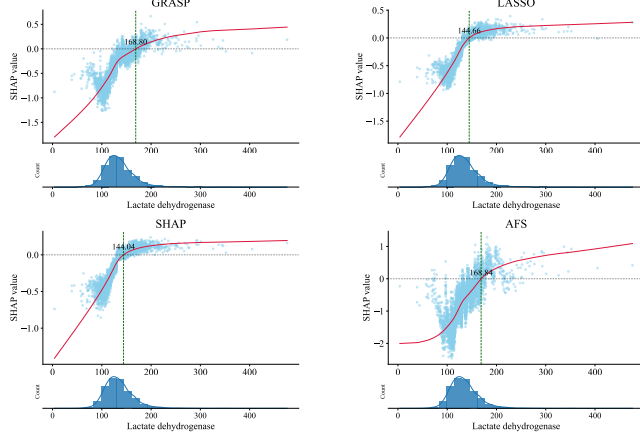


Fig. 2: Main effect plots of Lactate dehydrogenase (LDH) using overlapping feature sets from GRASP, LASSO, SHAP and AFS. Red curves depict LOWESS curves and blue dots show Shapley values. Histograms indicate LDH distribution, and dashed lines mark estimated thresholds across methods.

3.1. Experiments Setup

Datasets. We used two datasets. The development dataset was NHANES (National Health and Nutrition Examination Survey) [17], a biennial US survey combining interviews, physical examinations, and laboratory tests. We used 1999–2014 cycles, restricted to adults (≥ 20 years) with mortality follow-up through December 31, 2019. Variables with $>10\%$ missingness were removed. All-cause mortality were obtained from the linked mortality file. UK Biobank (UKB) [18] served as external validation (accessed under Application Number 240523), with 15,082 participants and confirmed 5-year mortality (before July 2024). To assess generalizability of features selected by different feature selection methods, 76 variables (86 after encoding) overlapped between NHANES and UKB were used. For more details regarding data processing and targeted patients, please visit <https://github.com/yhluo7/GRASP>.

Baselines. We compared GRASP with LASSO, SHAP method, and the AFS algorithm [19]. For LASSO, the penalty parameter was tuned by five-fold cross-validation. For SHAP, per-feature Shapley values were aggregated and features

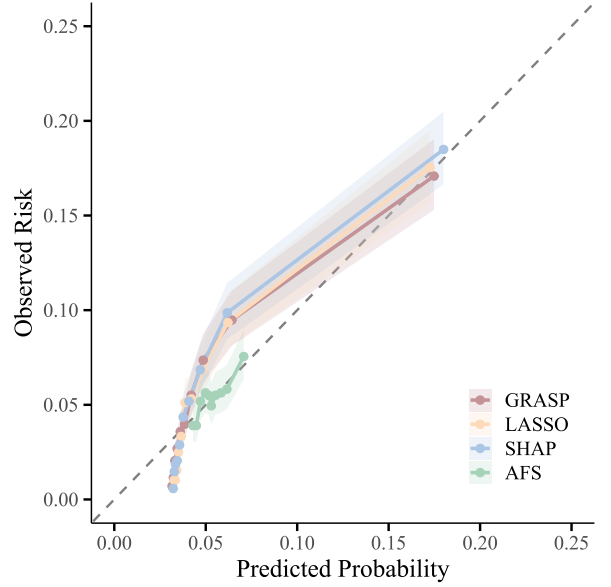


Fig. 3: Calibration curve comparing predicted probabilities and observed risks for models based on feature sets from GRASP, LASSO, SHAP, and AFS. All results are calibrated using the Platt Scaling method. The dashed line indicates perfect calibration, with shaded areas representing 95% confidence intervals.

above the median value were retained. AFS was run with default settings. To avoid data leakage, preprocessing procedure was fitted on training fold and applied on validation fold: (1) one-hot encoding of categorical variables; (2) median and mode imputation; (3) z-score standardization of continuous features.

Evaluation metrics. We assessed feature selection by predictability (Accuracy, F1 score, and Matthews correlation coefficient (MCC)), redundancy (average Variance Inflation Factor (VIF), Shapley value [20] and Pearson correlation coefficient), and stability (Jaccard Index (JI) and the Adjusted Stability Measure (ASM) [21]). We applied 1,000 bootstrap iterations on the NHANES validation set and UKB dataset to obtain reliable estimates. We also use calibration curves and Kaplan–Meier survival curves to evaluate the risk estimation and stratification ability of different selected features by training a COX model on the UKB dataset.

Implementation details. We first split the NHANES dataset into training and validation sets with an 80:20 ratio. For each feature selection method, we restricted the analysis to the 76 features shared with UKB and performed five-fold partitioning within the NHANES training set. Features consistently selected across all five folds were retained as the final feature set for that method. Based on the selected features, we trained logistic regression, random forests and XGBoost models, tuning their hyperparameters on the training set using

Table 1: Comparison of feature predictive performance on NHANES and UKB datasets. Other results are statistically significant at the 5% level compared with the GRASP method. The best score for each metric within a dataset is highlighted in bold. A dash indicates that the model predicted all samples as negative under the default probability threshold of 0.5.

Model	Metric	NHANES				UKB			
		GRASP	LASSO	SHAP	AFS	GRASP	LASSO	SHAP	AFS
LR	Accuracy	0.783	0.786	0.785	0.650	0.755	0.752	0.735	0.704
LR	F1	0.483	0.491	0.487	0.283	0.197	0.203	0.206	0.120
LR	MCC	0.436	0.448	0.440	0.155	0.170	0.181	0.191	0.050
RF	Accuracy	0.890	0.884	0.883	0.878	0.946	0.946	0.945	0.946
RF	F1	0.226	0.120	0.093	—	0.016	0.007	0.009	—
RF	MCC	0.297	0.206	0.186	—	0.045	0.032	0.048	—
XGB	Accuracy	0.897	0.895	0.886	0.878	0.942	0.940	0.937	0.946
XGB	F1	0.437	0.431	0.393	—	0.143	0.137	0.152	—
XGB	MCC	0.416	0.406	0.356	—	0.142	0.150	0.142	—

Table 2: Comparison of different feature selection methods and redundancy on the NHANES dataset. For LASSO and SHAP, the selected features exhibited multicollinearity, therefore the corresponding results are denoted with a dash. P<0.05:*, P<0.01:**, P<0.001:***.

Metric	GRASP	LASSO	SHAP	AFS
Feature number	23	44**	43***	59
Adjusted stability measure	0.593	0.382***	0.398***	0.258***
Shapley Value	0.101	0.074***	0.085**	0.054***
VIF	2.942	—	—	8.201
Correlation	0.070	0.079**	0.082**	0.064

Optuna [22]. Model performance was then evaluated on the validation set and UKB through 1,000 bootstrap resamples to compare the ability of feature sets.

3.2. Performance evaluation

Results in Tables 1 and 2 and Figures 2 to 4 highlight that GRASP identified the least feature set (23 features on average) with the highest stability (0.593) and lowest redundancy (VIF = 2.942), effectively avoiding the multicollinearity observed in LASSO and SHAP. Moreover, features selected by GRASP maintained predictive performance comparable to larger feature sets across NHANES and UKB. Calibration and Kaplan-Meier analyses further confirmed its robustness. GRASP’s calibration curve aligned more closely with observed risks in high-risk groups, and its Kaplan-Meier stratification achieved equal or better discrimination than two other methods. For interpretability, focusing on Lactate dehydrogenase (LDH, selected by all methods), GRASP produced a LOWESS curve whose transition point (168.8 U/L) was closest to the clinical cutoff reported by Guo et al. (315 U/L)[23], compared with 144.66 U/L for LASSO, 144.04 U/L for SHAP. AFS shares a similar threshold (168.84 U/L), but shows a sharper SHAP increase before it. Overall, GRASP aligns best with prior clinical evidence and yields the most

interpretable features.

4. CONCLUSION

We develop a feature-selection method that combines L_{21} norm with SHAP-based interpretability. Experiments on real-world datasets confirm its competitive performance compared with existing feature selection methods. Future studies could improve efficiency on high-dimensional datasets.

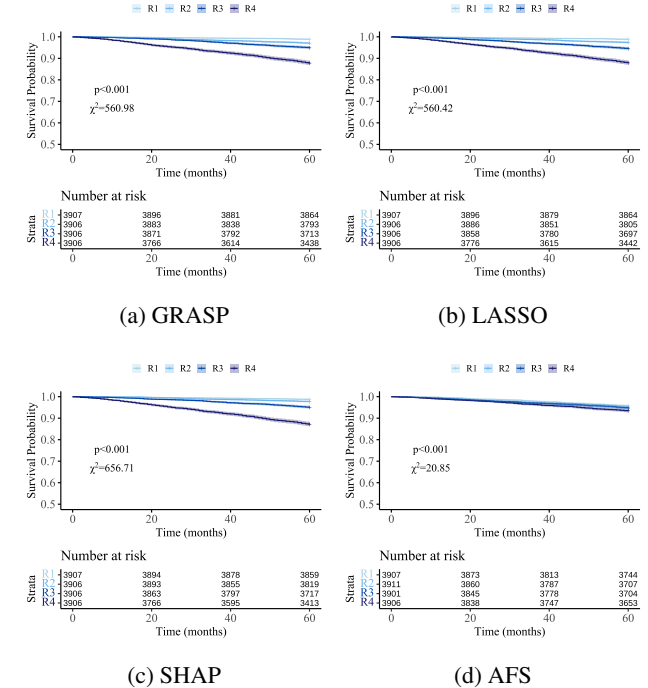


Fig. 4: Comparison of different feature selection methods using Kaplan-Meier curves in the UKB dataset. Confidence bands represent the 95% confidence interval. The global log-rank test and test statistic are reported in each Kaplan-Meier plot.

5. ACKNOWLEDGMENT

The work was supported by the Noncommunicable Chronic Diseases–National Science and Technology Major Project (Project Number 2023ZD0506000). The funders had no role in study design, data collection and analysis, decision to publish, or preparation of the manuscript.

6. COMPLIANCE WITH ETHICAL STANDARDS

This study was conducted retrospectively using human subject data made available publicly by NHANES and the UK Biobank (accessed under application number 240523). Ethical approval was not required as confirmed by the license attached with the public data.

7. REFERENCES

- [1] F. Wang, L. P. Casalino, and D. Khullar, “Deep learning in medicine—promise, progress, and challenges,” *JAMA Intern. Med.*, vol. 179, pp. 293–294, 2019.
- [2] I. Guyon, S. Gunn, M. Nikravesh, et al., *Feature extraction: foundations and applications*, vol. 207, Springer, 2008.
- [3] J. Gui, Z. Sun, S. Ji, et al., “Feature selection based on structured sparsity: A comprehensive study,” *IEEE Trans. Neural Netw. Learn. Syst.*, vol. 28, pp. 1490–1507, 2016.
- [4] J. Li, K. Cheng, S. Wang, et al., “Feature selection: A data perspective,” *ACM Comput. Surv.*, vol. 50, pp. 1–45, 2017.
- [5] G. Chandrashekhar and F. Sahin, “A survey on feature selection methods,” *Comput. Electr. Eng.*, vol. 40, pp. 16–28, 2014.
- [6] R. Kohavi and G. H. John, “Wrappers for feature subset selection,” *Artif. Intell.*, vol. 97, pp. 273–324, 1997.
- [7] J. Tang, S. Alelyani, and H. Liu, “Feature selection for classification: A review,” *Data Classification: Algorithms and Applications*, p. 37, 2014.
- [8] R. Tibshirani, “Regression shrinkage and selection via the lasso,” *J. R. Stat. Soc. Ser. B Methodol.*, vol. 58, pp. 267–288, 1996.
- [9] S. Rey, E. Curbelo, L. Martino, et al., “Enhancing graphical lasso: A robust scheme for non-stationary mean data,” *arXiv preprint arXiv:2503.19651*, 2025.
- [10] T. Chen and C. Guestrin, “Xgboost: A scalable tree boosting system,” in *Proc. 22nd ACM SIGKDD*, 2016, pp. 785–794.
- [11] M. Marinescu, G. Villacrés, L. Martino, et al., “Scoring functions to evaluate the rankings methods for variable selection,” in *EUSIPCO*, 2025.
- [12] R. San Millán-Castillo, L. Martino, E. Morgado, et al., “An exhaustive variable selection study for linear models of soundscape emotions: Rankings and gibbs analysis,” *IEEE/ACM TASLP*, vol. 30, pp. 2460–2474, 2022.
- [13] U. M. Khaire and R. Dhanalakshmi, “Stability of feature selection algorithm: A review,” *J. King Saud Univ. Comput. Inf. Sci.*, vol. 34, pp. 1060–1073, 2022.
- [14] M. Ghassemi, T. Naumann, P. Schulam, et al., “A review of challenges and opportunities in machine learning for health,” *AMIA Summit Transl. Sci. Proc.*, vol. 2020, pp. 191, 2020.
- [15] L. Armijo, “Minimization of functions having lipschitz continuous first partial derivatives,” *Pac. J. Math.*, vol. 16, pp. 1–3, 1966.
- [16] R. Vershynin, “Introduction to the non-asymptotic analysis of random matrices,” in *Compressed Sensing: Theory and Applications*, pp. 210–268. Cambridge University Press, 2012.
- [17] V. K. Nguyen, L. Y. Middleton, L. Huang, et al., “Harmonized us national health and nutrition examination survey 1988–2018 for high throughput exposome-health discovery,” *MedRxiv*, 2023.
- [18] C. Sudlow, J. Gallacher, N. Allen, et al., “Uk biobank: an open access resource for identifying the causes of a wide range of complex diseases of middle and old age,” *PLoS Med.*, vol. 12, pp. e1001779, 2015.
- [19] N. Gui, D. Ge, Z. Hu, et al., “Afs: An attention-based mechanism for supervised feature selection,” in *AAAI*, 2019, vol. 33, pp. 3705–3713.
- [20] S. M. Lundberg and S. I. Lee, “A unified approach to interpreting model predictions,” *Adv. Neural Inf. Process. Syst.*, vol. 30, 2017.
- [21] J. L. Lustgarten, V. Gopalakrishnan, and S. Visweswaran, “Measuring stability of feature selection in biomedical datasets,” in *Proc. AMIA Annu. Symp.*, 2009, vol. 2009, p. 406.
- [22] T. Akiba, S. Sano, T. Yanase, et al., “Optuna: A next-generation hyperparameter optimization framework,” in *Proc. ACM SIGKDD Int. Conf. Knowl. Discov. Data Min.*, 2019, pp. 2623–2631.
- [23] P. Guo, H. Ding, X. Li, et al., “Association between lactate dehydrogenase levels and all-cause mortality in icu patients with heart failure: a retrospective analysis of the mimic-iv database,” *BMC Cardiovasc. Disord.*, vol. 25, pp. 62, 2025.